ELSEVIER

Journal of Alloys and Compounds 323–324 (2001) 408–411

Journal of ALLOYS AND COMPOUNDS

www.elsevier.com/locate/jallcom

Phase segregation and orbital ordering in $Bi_{1-x}Ca_xMnO_3$ ($x \geq 0.75$): a neutron and synchrotron X-ray diffraction study

J.L. García-Muñoz[a,*], M.A.G. Aranda[b], A. Llobet[a,c], C. Frontera[a], M.J. Martínez-Lope[d], C. Ritter[e], M. Respaud[f], J.M. Broto[f]

[a]*Institut de Ciencia de Materials de Barcelona, CSIC, Campus de la UAB, E-08193 Bellaterra, Spain*
[b]*Departamento de Química Inorgánica, Cristalografía y Mineralogía, Universidad de Málaga, 29071 Málaga, Spain*
[c]*Lab. Louis Néel, CNRS, 25 Avenue des Martyrs, BP 166, 38042 Grenoble Cedex, France*
[d]*Instituto de Ciencia de Materiales de Madrid, CSIC, Madrid, Spain*
[e]*Institut Laue–Langevin, 38042 Grenoble Cedex, France*
[f]*SNCMP and LPMC, INSA, Complexe Scientifique de Rangueil, Toulouse 31077, France*

Abstract

High-resolution synchrotron X-ray and neutron powder diffraction of $Bi_{1-x}Ca_xMnO_3$ ($x \geq 0.75$) has shown that these systems present a phase segregation coinciding with the electronic localization of the e_g electrons. The very precise results obtained provide evidence of a mechanism for phase segregation based on subtle compositional heterogeneity effects.

Keywords: Crystal structure and symmetry; Magnetically ordered materials; Electron–phonon interactions

PACS: 71.45.Lr; 71.38.+i; 71.27. +a; 75.25.+z; 71.30.+h

1. Introduction

The rich phenomena associated to the structural, magnetic and electronic transitions in manganese oxides with perovskite-type structure ($Ln_{1-x}A_xMnO_3$ with Ln, lanthanide; A, alkaline earth) have been the subject of a large research effort. As a consequence of the two-fold degeneracy of the e_g electrons and the competition several interactions, a large variety of ground states are found in this family of compounds. Besides the ferromagnetic double exchange interaction, the Coulomb repulsion and Jahn–Teller tendencies favor localization of the charges. Colossal-magneto-resistance CMR [1] and metal–insulator transitions, associated with the real space orbital (and charge) ordering/disordering phenomena, are found at several doping levels in these oxides. The discovery of CMR has led to an explosion of interest in the tendency displayed by many manganites, and other transition metal oxides, to form inhomogeneous/segregated states. It is important to distinguish between nanoscopic phase segregation (electronic phase separation, stripes and charge-ordering phenomena in general) [2], where the length scales are of the order of 3–20 Å, from macroscopic phase separation, where the length scales are larger than 1000 Å [3]. The strong relationship between CMR and phase separation makes nanoscopic and macroscopic phase segregation a current hot topic that deserves attention.

As part of a systematic investigation of the $Bi_{1-x}A_xMnO_3$ family of manganites, in this work we focus on the range of the highly doped region that displays CMR properties ($x \geq 0.75$). Low temperature phase segregation phenomena have been observed in most of the specimens investigated in this portion of the phase diagram. We present a study based on high-energy synchrotron X-ray (SXRPD) and neutron powder diffraction (NPD).

2. Experimental

The compositions $x = 0.85$ and 0.875 were selected because they are respectively, at each side of the boundary that separates the appearance of long range ferromag-

*Corresponding author.
E-mail address: garcia.munoz@icmab.es (J.L. García-Muñoz).

0925-8388/01/$ – see front matter
PII: S0925-8388(01)01098-2

netism. Polycrystalline $Bi_{1-x}Ca_xMnO_3$, $x = 0.85$ and 0.875, powders were prepared by standard solid state ceramic synthesis in air with several mechano-thermal cycles to ensure sample homogeneity. The starting compounds were Bi_2O_3, $CaCO_3$ and MnO_2. The stoichiometric mixtures were first heated at 1000°C several times with intermediate grinding. Finally, in the form of pellets, samples were annealed at 1250°C for 24 h several times. Heating and cooling rates were 300°C/h. The $x = 0.75$ specimen was synthesized under oxygen pressure. In this brief communication we will mainly focus on the $x = 0.85$ sample. Further details about the other two will be published elsewhere.

High-resolution SXRPD patterns were recorded on the BM16 powder diffractometer at ESRF (Grenoble, France) [4] in Debye–Scherrer (transmission) configuration at $T =$ 300 and 10 K. The samples were loaded into a borosilicate glass capillary ($\phi = 0.5$ mm) and rotated during data collection. A short wavelength, $\lambda = 0.442377(2)$ Å ($\approx$28.03 keV), was selected with a double-crystal Si(111) monochromator and calibrated with Si NIST. Each run took about 3.5 h to obtain good statistics over the 2θ angular range of 4 to 38°; the data from the detectors were normalized and summed to 0.004° step size. NPD measurements were performed at the Institute Laue–Langevin in Grenoble. Neutron data for $Bi_{0.15}Ca_{0.85}MnO_3$ were collected on the high-resolution D2B diffractometer ($\lambda =$ 1.594 Å) in the high-flux mode at 2 and 300 K. A high-intensity D20 diffractometer ($\lambda = 2.42$ Å) was used to obtain a better resolution in the low 2θ angular range, especially suitable for investigating magnetic structures. D20 data were collected at various temperatures between 1.5 and 300 K. NPD data were always collected during a warming up process. Structural and magnetic parameters were refined by the Rietveld method using the programs FULLPROF [5] and GSAS [6]. Combined NPD and SXRD refinements were performed on $Bi_{0.15}Ca_{0.85}MnO_3$ at 10 and 300 K. Pulsed high field measurements were performed at SNCMP (Toulouse, France).

3. Results and discussion

The crystal structure of the $x = 0.85$ and 0.875 samples at RT corresponds to the *Pnma* (or *Pbnm*) type symmetry. A minor phase, $CaMn_2O_4$ [refined weight ratio of 3.6(1) and 4.8(1) %, respectively], was detected and accounted for appropriately. Refining the atomic coefficients, positional and isotropic thermal parameters, with the nominal composition for $Bi_{0.15}Ca_{0.85}MnO_3$, did not yield a completely satisfactory refinement because some peaks did not have adequate intensity (see Fig. 1). As this was a joint refinement of SXRPD and NPD data, we were able to freely refine the occupation factors of Bi and Ca without constraints. Optimization of the Mn occupation factor did not improve the fit and this parameter was set to 1.0. But the occupation factor of Ca converged to 0.75(1), yielding the correct intensity for the aforementioned peaks. Hence, $Bi_{0.15}$-O-HT is non-stoichiometric with calcium vacancies (~8%) at the A site. The final joint refinement converged to $R_{WP} = 3.52$ and $R_F = 2.25\%$ for the SXRPD data and to $R_{WP} = 5.04$ and $R_F = 1.80\%$ for the NPD data. Details of the refined parameters, including anisotropic broadening, are given elsewhere [7].

At low temperature the existence of a structural phase transition was apparent. The SXRPD pattern of $Bi_{0.15}Ca_{0.85}MnO_3$ at 10 K is very complex, as shown in Figs. 2 and 3 (SXRPD and NPD, in the same d-spacing region, respectively). A detailed inspection indicated the coexistence of the pristine orthorhombic phase ($Bi_{0.15}$-O-LT) and a new monoclinic phase ($Bi_{0.15}$-M-LT), plus the $CaMn_2O_4$ impurity. A $P2_1/m$ low temperature phase was previously reported in other manganites with the same doping level [8]. The final joint refinement was $R_{WP} =$ 4.16%, $R_F^{O\text{-}LT} = 2.12\%$ and $R_F^{M\text{-}LT} = 2.23\%$ for the SXRPD data and $R_{WP} = 5.48\%$, $R_F^{O\text{-}LT} = 1.84\%$ and $R_F^{M\text{-}LT} = 1.91\%$ for the NPD data.

The refined weight fractions were: 67.7(6) % $Bi_{0.15}$-M-LT, 28.8(3) % $Bi_{0.15}$-O-LT and 3.5(1) % $CaMn_2O_4$. The evolution of the LT $P2_1/m$ and HT *Pnma* cell parameters

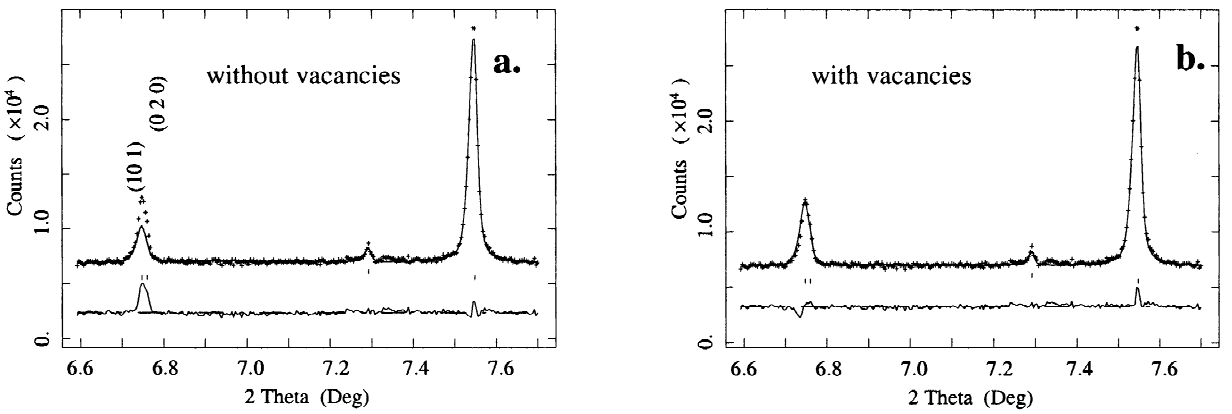

Fig. 1. Selected region of the SXRPD Rietveld plot for $Bi_{0.15}Ca_{0.85}MnO_3$ at 300 K with (a) nominal stoichiometry and (b) freely refining the occupation factors of the cations at the A site of the perovskite.

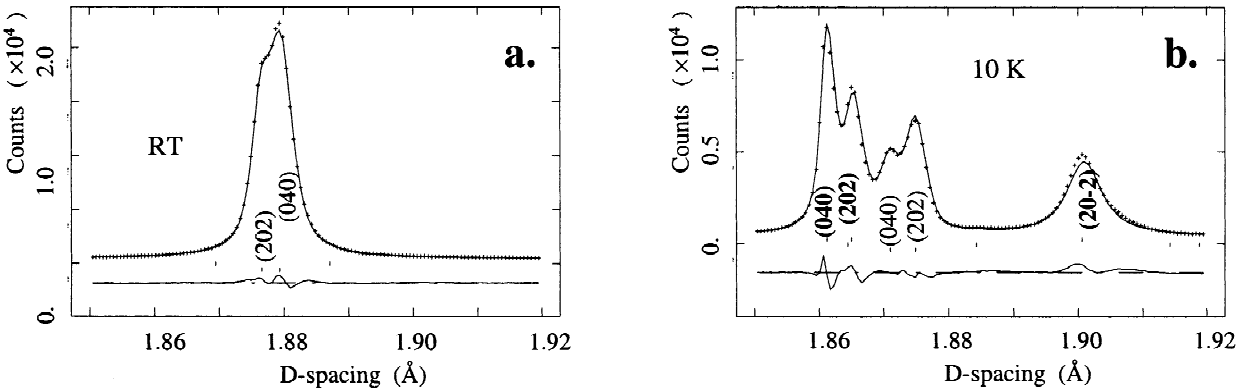

Fig. 2. Selected region, 1.85–1.92 Å, of the SXRPD Rietveld plot for '$Bi_{0.15}Ca_{0.85}MnO_3$' at (a) 300 K and (b) 10 K. Reflections indexed in bold correspond to the $Bi_{0.15}$-M-LT phase.

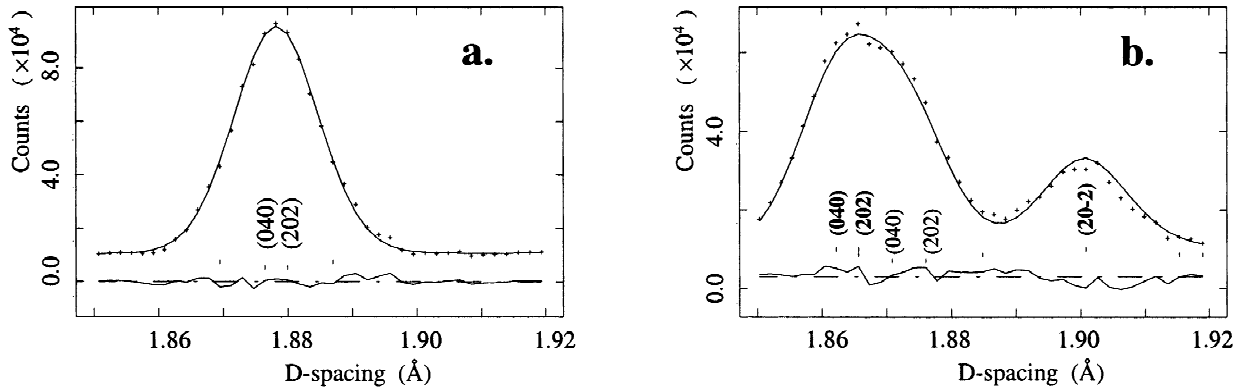

Fig. 3. Selected region, 1.85–1.92 Å, of the NPD Rietveld plot for '$Bi_{0.15}Ca_{0.85}MnO_3$' at (a) 300 K and (b) 10 K. Reflections indexed in bold correspond to the $Bi_{0.15}$-M-LT phase.

was determined from the medium resolution NPD patterns (Fig. 4). Moreover, NPD data evidenced two sets of magnetic peaks with respective propagation vectors $\boldsymbol{k} = (1/2\ 0\ 1/2)$ and $(0\ 1\ 0)$ below $T_N = 125(2)$ K, coinciding with the electronic localization. $Bi_{0.15}$-O-LT displays a G-type magnetic structure [9] characterized by an antiferromagnetic (AFM) coupling between neighboring Mn ions along the three directions of the pseudocubic axis [$\boldsymbol{k} = (0\ 1\ 0)$, $m_y = 1.24\ \mu_B$/Mn at 1.5 K]. This is the spin ordering of orthorhombic $CaMnO_3$ with $T_N = 122$ K and 100% Mn^{4+}. At this composition the dominant magnetic interaction is the AFM superexchange between t_{2g} orbitals leading to the G-type magnetic structure. A particular case of the C-type [9,10] magnetic structure appears in the $Bi_{0.15}$-M-LT phase below $T_N \sim 125$ K. The particular order found can be explained through the OO depicted in Fig. 5. A detailed analysis of the stability of this OO vs. field will be reported elsewhere. This highly anisotropic OO also explains the thermal behavior seen in Fig. 4. This OO is characterized by the localization of the e_g electrons in $d_{3z^2-r^2}$ orbitals polarized along the $(1\ 0\ -1)$ direction forming one-dimensional metallic bands that are perpendicular to the AFM planes depicted in Fig. 5.

A central result of this work is related to the mechanism that explains the phase segregation on cooling. Only two possibilities can be considered: (i) both phases are present at RT, but they are masked, even to the ultra-high-resolution SXRPD; or (ii) a single homogeneous non-stoi-

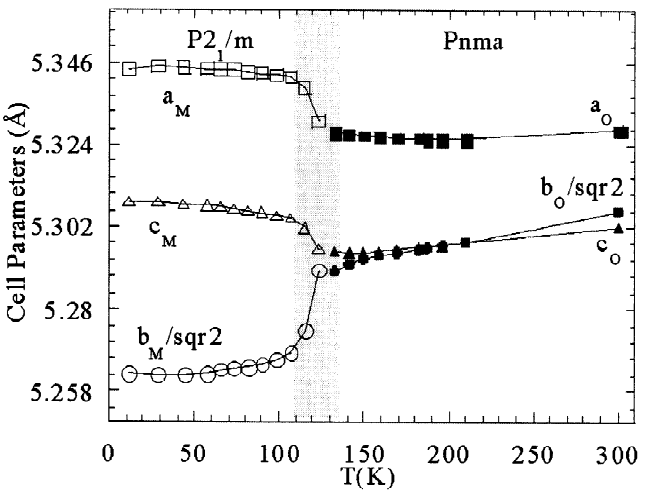

Fig. 4. Temperature dependence of the lattice parameters for the LT monoclinic phase.

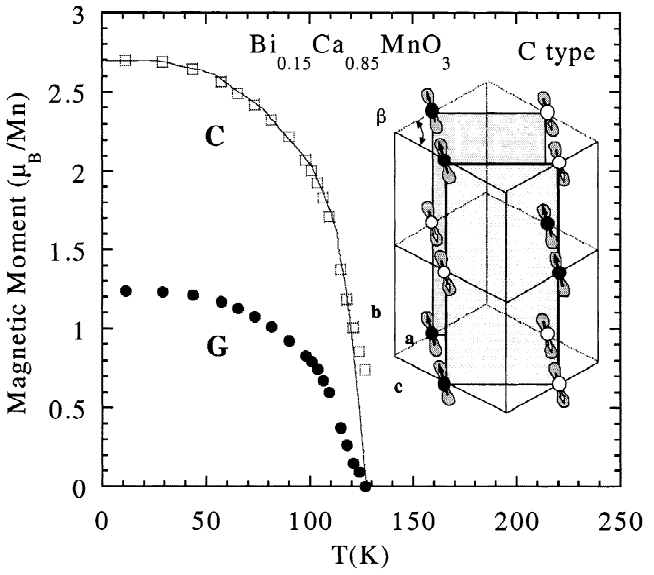

Fig. 5. Temperature dependence of the C-type ordered moments obtained from NPD data for $Bi_{0.15}Ca_{0.85}MnO_3$. Schematic diagram of the ordering of the e_g occupied orbitals in the $P2_1/m$ cell.

chiometric phase is present at RT, but large strains develop between the nucleation centers and the pristine bulk material, which prevents complete transformation of the sample.

Our high-resolution data and joint refinement indicate that the first explanation, chemical heterogeneity, is the correct one. The Rietveld refinement converged to different cation stoichiometries for $Bi_{0.15}$-M-LT and $Bi_{0.15}$-O-LT. $Bi_{0.15}$-O-LT is almost stoichiometric [Ca: 0.89(3), G type] and the calcium vacancies are concentrated in $Bi_{0.15}$-M-LT [Ca: 0.68(3), G type]. In addition, it is important to emphasize that, if the strain between the domains is the key parameter, then the microstrain terms of $Bi_{0.15}$-O-HT should be smaller than strained $Bi_{0.15}$-O-LT, which is not the case [7]. Conversely, the peaks of $Bi_{0.15}$-O-LT are sharper than those of $Bi_{0.15}$-O-HT. So, this macroscopic phase segregation, commonly found in many manganites, is not the result of atom diffusion or strain development but a structural consequence of the chemical heterogeneity of the sample. Such chemical heterogeneity must also be present at RT, but it does not produce, up to the present (very high) resolution, two distinguishable cells. Only the structural distortion associated with the charge localization and induced by the onset of the OO produced measurable differences between the two present phases. Increasing the Ca content, the proportion of the two phases found in nominal $Bi_{0.125}Ca_{0.875}MnO_3$ at 10 K were 84.7 and 15.2% for the $P2_1/m$ and *Pnma* cells, respectively.

In summary, high-resolution synchrotron X-ray powder diffraction and high-resolution neutron powder diffraction of $Bi_{1-x}Ca_xMnO_3$ ($x \geq 0.75$) show that these systems present a phase segregation coinciding with the electronic localization of the e_g electrons and the onset of particular orbital ordering. The very precise results obtained provide evidence of a mechanism for phase segregation based on subtle compositional heterogeneity effects.

Acknowledgements

Financial support from CICyT (MAT97-0699), MEC (PB97-1175), Generalitat de Catalunya (GRQ95-8029) and the EC through the 'Oxide Spin Electronics (OXSEN)' network (TMR) is gratefully acknowledged. Provision of the beam time at the ILL (neutrons) and ESRF (synchrotron X-rays) facilities is acknowledged.

References

[1] S. Jin et al., Sience 264 (1994) 413.
[2] A. Moreo, S. Yunoki, E. Dagotto, Science 283 (1999) 2034.
[3] P. Littlewood, Nature 399 (1999) 529.
[4] M.A.G. Aranda, J.P. Attfield, Angew. Chem. Int. Ed. Engl. 32 (1993) 1454.
[5] J. Rodríguez-Carvajal, Physica B 192 (1993) 55.
[6] A.C. Larson, R.B. von Dreele, Version PC-98, Los Alamos National Laboratory Report No. LA-UR-86-748, 1994.
[7] A. Llobet, C. Frontera, J.L. García-Muñoz, C. Ritter, M.A.G. Aranda, Chem. Mater. 12 (2000) 3648.
[8] C. Martin, A. Maignan, M. Hervieu, B. Raveau, Z. Jirák, A. Kurbakov, V. Trounov, G. Andre, F. Bouree, J. Magn. Magn. Mater. 205 (1999) 184.
[9] E.O. Wollan, W.C. Koehler, Phys. Rev. 100 (1955) 545.
[10] A. Llobet, J.L. García-Muñoz, C. Frontera, C. Ritter, Phys. Rev. B 60 (1999) 9889.